Geophysical Fluid Dynamics Laboratory general circulation model investigation of the indirect radiative effects of anthropogenic sulfate aerosol

Yi Ming

Visiting Scientist Program, University Corporation for Atmospheric Research, Geophysical Fluid Dynamics Laboratory, Princeton, New Jersey, USA

V. Ramaswamy, Paul A. Ginoux, and Larry W. Horowitz

Geophysical Fluid Dynamics Laboratory, Princeton, New Jersey, USA

Lynn M. Russell

Scripps Institution of Oceanography, University of California, San Diego, La Jolla, California, USA

Received 30 April 2005; accepted 19 July 2005; published 29 November 2005.

[1] The Geophysical Fluid Dynamics Laboratory (GFDL) atmosphere general circulation model, with its new cloud scheme, is employed to study the indirect radiative effect of anthropogenic sulfate aerosol during the industrial period. The preindustrial and present-day monthly mean aerosol climatologies are generated from running the Model for Ozone And Related chemical Tracers (MOZART) chemistry-transport model. The respective global annual mean sulfate burdens are 0.22 and 0.81 Tg S. Cloud droplet number concentrations are related to sulfate mass concentrations using an empirical relationship (Boucher and Lohmann, 1995). A distinction is made between "forcing" and flux change at the top of the atmosphere in this study. The simulations, performed with prescribed sea surface temperature, show that the first indirect "forcing" ("Twomey" effect) amounts to an annual mean of -1.5 W m^{-2}, concentrated largely over the oceans in the Northern Hemisphere (NH). The annual mean flux change owing to the response of the model to the first indirect effect is -1.4 W m^{-2}, similar to the annual mean forcing. However, the model's response causes a rearrangement of cloud distribution as well as changes in longwave flux (smaller than solar flux changes). There is thus a differing geographical nature of the radiation field than for the forcing even though the global means are similar. The second indirect effect, which is necessarily an estimate made in terms of the model's response, amounts to -0.9 W m^{-2}, but the statistical significance of the simulated geographical distribution of this effect is relatively low owing to the model's natural variability. Both the first and second effects are approximately linearly additive, giving rise to a combined annual mean flux change of -2.3 W m^{-2}, with the NH responsible for 77% of the total flux change. Statistically significant model responses are obtained for the zonal mean total indirect effect in the entire NH and in the Southern Hemisphere low latitudes and midlatitudes (north of 45°S). The area of significance extends more than for the first and second effects considered separately. A comparison with a number of previous studies based on the same sulfate-droplet relationship shows that, after distinguishing between forcing and flux change, the global mean change in watts per square meter for the total effect computed in this study is comparable to existing studies in spite of the differences in cloud schemes.

Citation: Ming, Y., V. Ramaswamy, P. A. Ginoux, L. W. Horowitz, and L. M. Russell (2005), Geophysical Fluid Dynamics Laboratory general circulation model investigation of the indirect radiative effects of anthropogenic sulfate aerosol, *J. Geophys. Res.*, *110*, D22206, doi:10.1029/2005JD006161.

1. Introduction

[2] Aerosol particles are necessary for cloud formation in the atmosphere. In meteorological conditions favorable for supersaturation (i.e., relative humidity is over 100%), excess water vapor condenses onto aerosol particles in large

0148-0227/05/2005JD006161$09.00

Table 1. Summary on Existing Studies of Indirect Effects Using the Relationship of *Boucher and Lohmann* [1995]

	Cloud Scheme			Sulfate Burden, Tg S		Flux Changes due to Indirect Effects, W m^{-2}		
	Cloud Water	Cloud Amount	Autoconversion	PI	PD	First	Second	Combined
Boucher and Lohmann [1995]	*Le Treut and Li* [1991]	*Le Treut and Li* [1991]	*Boucher et al.* [1994][a]	0.34	0.78	−1.0		
Boucher and Lohmann [1995]	*Sundqvist* [1978]; *Roeckner et al.* [1991]	*Sundqvist et al.* [1989]	*Sundqvist* [1978]; *Smith* [1990]	0.34	0.78	−1.0		
Feichter et al. [1997][b]	*Lohmann and Roeckner* [1996]	*Sundqvist et al.* [1989]	*Beheng* [1994]	0.3	0.68	−0.8		
Lohmann and Feichter [1997][c]	*Lohmann and Roeckner* [1996]	*Sundqvist et al.* [1989]	*Beheng* [1994]	0.36	1.05	−1.0		−1.4
Lohmann and Feichter [1997][c]	*Lohmann and Roeckner* [1996]	*Xu and Randall* [1996]	*Beheng* [1994]	0.34	0.96			−4.8
Lohmann and Feichter [1997][c]	*Lohmann and Roeckner* [1996]	*Xu and Randall* [1996]	*Berry* [1967]	0.32	0.89			−2.2
Rotstayn [1999]	*Smith* [1990]; *Rotstayn* [1997]	*Smith* [1990]; *Rotstayn* [1997]	*Manton and Cotton* [1977]	0.21	0.51	−1.2	−1.0	−2.1
Kiehl et al. [2000]	*Rasch and Kristjánsson* [1998]	*Rasch and Kristjánsson* [1998]	*Chen and Cotton* [1987]		0.37[d]	−1.8		
Rotstayn and Penner [2001]	*Smith* [1990], *Rotstayn* [1997], *Rotstayn et al.* [2000]	*Smith* [1990], *Rotstayn* [1997], *Rotstayn et al.* [2000]	*Rotstayn* [2000]	0.20	0.50	−1.5	−1.3	−2.6
This study	*Tiedtke* [1993]	*Tiedtke* [1993]	*Khairoutdinov and Kogan* [2000]	0.22	0.81	−1.4	−0.9	−2.3

[a]Precipitation was parameterized according to *Boucher et al.* [1994].
[b]Cloud physics does not affect simulated sulfate concentrations.
[c]Model simulation of sulfate concentrations is coupled to cloud physics.
[d]*Kiehl et al.* [2000] reported an annual mean anthropogenic sulfate burden of 0.37 Tg S.

amount and grows some of them into cloud droplets. Since water droplets are efficient in scattering sunlight, clouds play an important role in the Earth's radiation balance. As highly efficient cloud condensation nuclei (CCN), anthropogenic aerosols such as sulfate aerosol affect cloud properties through increasing droplet numbers. The elevated droplet numbers have a tendency to decrease droplet radii (the first indirect effect or "Twomey" effect) and lengthen cloud lifetime (the second indirect effect or "Albrecht" effect). Both effects may profoundly alter radiative forcing, and hence have the potential to affect climate.

[3] In the past decade, a number of studies have been devoted to better understanding the indirect radiative effects of aerosols. Most of them involved global simulations using various general circulation models (GCMs). Since the core issues surrounding the indirect effects lie right at the heart of aerosol-cloud interactions, a GCM ideal for exploring them ought to excel at representing three key processes, namely the formation of cloud water, physical and chemical evolution of aerosols, and cloud droplet activation.

[4] GCMs normally describe clouds in terms of cloud water (liquid, ice or a mixture of both) and cloud amount (the cloudy fraction of a GCM grid box). The Geophysical Fluid Dynamics Laboratory (GFDL) AM2 GCM has implemented a prognostic cloud scheme by explicitly accounting for sources and sinks of water substance. The cloud microphysical processes involved are parameterized to different extents as constrained by the temporal and spatial resolutions of GCMs. Like other GCMs [e.g., *Boucher and Lohmann*, 1995; *Rotstayn*, 1999], the GFDL GCM makes use of monthly mean aerosol climatology, which is generated by running a chemistry-transport model off-line, to approximate the distributions of aerosols. A widely used empirical relationship links sulfate aerosol mass concentrations to droplet number concentrations [*Boucher and Lohmann*, 1995]. This study, as other prior ones, employs the same relationship, but differs from the previous studies in terms of the treatment of clouds and the aerosol climatology (Table 1) (see section 4 for a detailed comparison).

[5] The divergences among different GCM simulations of the indirect radiative effects of aerosols still persist because of inherent complexities of aerosol-cloud interactions [*Ramaswamy et al.*, 2001]. The estimated first indirect forcing varies from 0 to -1.5 W m^{-2}, while the range of the total flux changes due to the first and second indirect effects is even greater (e.g., -1.4 – -4.8 W m^{-2} as suggested by *Lohmann and Feichter* [1997]). One particular issue has been fitting the concept of "radiative forcing" to aerosol-cloud interactions beyond the first indirect effect. *Rotstayn and Penner* [2001] have, for example, used the term "quasi forcing" to go beyond the Twomey effect.

[6] In this GCM study of indirect effects, the treatment of some key aspects of aerosol-cloud interactions is described. We distinguish here between forcing (conforming to the IPCC definition) and flux changes which ensue when the model's climate responds to aerosol-cloud interactions. The radiative forcing and flux changes due to the first and second indirect effects are calculated along with an assessment of their signs, scales and geographical distributions. For the purposes of this study, we follow *Ramaswamy et al.* [2001] for the definition of "forcing" and consider only the first indirect effect to be a forcing. In contrast, the second

and the total indirect effects are regarded as involving a response in the climate variables. The feasibility of using flux change for estimating radiative forcing is assessed in light of the possibility of the response of the model. An important element of this study is the estimation of the statistical significance of the simulated global and zonal mean flux changes, accomplished by comparing with the model's unforced variations. It is noted that the different cases investigated and the manner of the GCM experiments described below are similar to those given by *Rotstayn* [1999] and *Rotstayn and Penner* [2001], albeit with different cloud and aerosol physics and a different GCM. Thus one purpose of this paper is to compare the results with both studies, as well as compare with other earlier works that focused on either the first or the total indirect effect.

2. Methodology

2.1. Model Description

[7] The GFDL atmosphere GCM AM2 is modified to simulate the roles of aerosols in affecting cloud properties and the resulting radiative effects. The horizontal resolution of the model is set at N45 (2.5° in longitude × 2° in latitude). Most of the 24 vertical model layers are in the troposphere. *The GFDL Global Atmospheric Model Development Team* [2004] provides a complete overview of the model structure and validation. Here we only briefly summarize some parts of the model that are most relevant to this study.

[8] The GCM employs the prognostic cloud scheme of *Tiedtke* [1993] to track cloud water and amount. The droplet number concentration is related to the mass concentration of sulfate aerosol via the empirical relationship of *Boucher and Lohmann* [1995]. The volume mean droplet radius is related to the effective droplet radius by a fixed ratio (1.077 for marine clouds and 1.143 for continental clouds) [*Martin et al.*, 1994]. The shortwave (SW) radiative properties of clouds are parameterized according to *Slingo* [1989]. Clouds in different model layers are assumed to be maximally overlapped if they are adjacent and to be randomly overlapped otherwise.

[9] The cloud microphysical processes except autoconversion are parameterized following *Rotstayn* [1997] and *Rotstayn et al.* [2000]. This study uses a continuous parameterization of autoconversion that is based on fitting cloud droplet size spectra from an explicit microphysical model [*Khairoutdinov and Kogan*, 2000]. Only water clouds are considered in this study since the possible mechanisms through which aerosols may affect ice cloud properties are not well understood, and the associated radiative effects are subject to large uncertainties [*Lohmann and Feichter*, 2004].

[10] The sulfate aerosol climatology used in this study is generated by interpolating the monthly mean results from the Model for Ozone And Related chemical Tracers (MOZART) [*Tie et al.*, 2001; *Horowitz et al.*, 2003; *Tie et al.*, 2005], a global chemistry-transport model that implements the interaction between tropospheric gas-phase species and aerosols. Driven by emissions and meteorology, the model is able to predict the spatially and temporally resolved mass concentrations of several types of aerosol. Aerosols are specified in the GCM grid boxes as off-line three-dimensional monthly mean fields. Aerosol concentrations are determined corresponding to emissions in 1860 (preindustrial or PI) and 1990 (present day or PD).

Table 2. Aerosol Climatology Used in Calculating the Cloud Droplet Number Concentration in Different Cases

	Aerosol Used in Radiation Scheme	Aerosol Used in Cloud Scheme
Case 1	PI	PI
Case 1a[a]	PD	PI
Case 2	PD	PI
Case 3	PI	PD
Case 4	PD	PD

[a]Model meteorology is the same as in case 1.

2.2. Experimental Design

[11] The GCM experiments performed here consist of five separate cases listed in Table 2: (1) Case 1 relates the droplet number concentration used in computing cloud optical depth in the radiation scheme, and in computing autoconversion and accretion rates in the cloud scheme, to the PI aerosol climatology. (2) Case 1a instantaneously switches the aerosol climatology used in the radiation scheme from PI to PD at every model time step, while keeping the meteorology the same as in case 1. (3) Case 2 feeds the radiation scheme with the PD aerosol climatology, while retaining the PI one for the cloud scheme. (4) Case 3 is opposite to case 2, using the PI and PD aerosol climatologies in the radiation and cloud schemes, respectively. (5) Case 4 uses the PD aerosol climatology in both schemes. Note that all of these cases fix the aerosol climatology at PI concentrations for clear-sky layers in the radiation calculation. This enables only the sensitivity due to aerosol-cloud interactions to be diagnosed. Each simulation spans a 11-year period, with the first year considered a spin-up. The evolution of the GCM's general circulation is forced by prescribed Atmospheric Model Intercomparison Project (AMIP) sea surface temperature (SST), and driven by the microphysical-radiation effects arising as a consequence of aerosol-cloud interactions.

[12] The difference between the various cases and case 1 reflects outcomes of particular microphysical-radiation interactions. We calculate the differences in total SW and longwave (LW) outgoing radiation flux at TOA at every radiation time step (3 hours) between cases 1 and 1a, and use the average flux change as an estimate of the first indirect forcing. The flux changes between cases 1 and 2 as well as between cases 1 and 3 are computed in the same way, and used to assess the first and second indirect effects, respectively, while those between cases 1 and 4 provide a measure of the combined first and second indirect effects.

[13] The experimental design here is similar to those of *Rotstayn* [1999] and *Rotstayn and Penner* [2001] in their fixed SST experiments. To the best of our knowledge, the present study appears to be the next one after those performed with the Commonwealth Scientific and Industrial Research Organization (CSIRO) GCM, in terms of similar experimental design, and using the diagnostic sulfate-droplet relationship to explore the first, second and total indirect effects in the context of prescribed SST. Thus this study offers a means to show the difference, if any, obtained

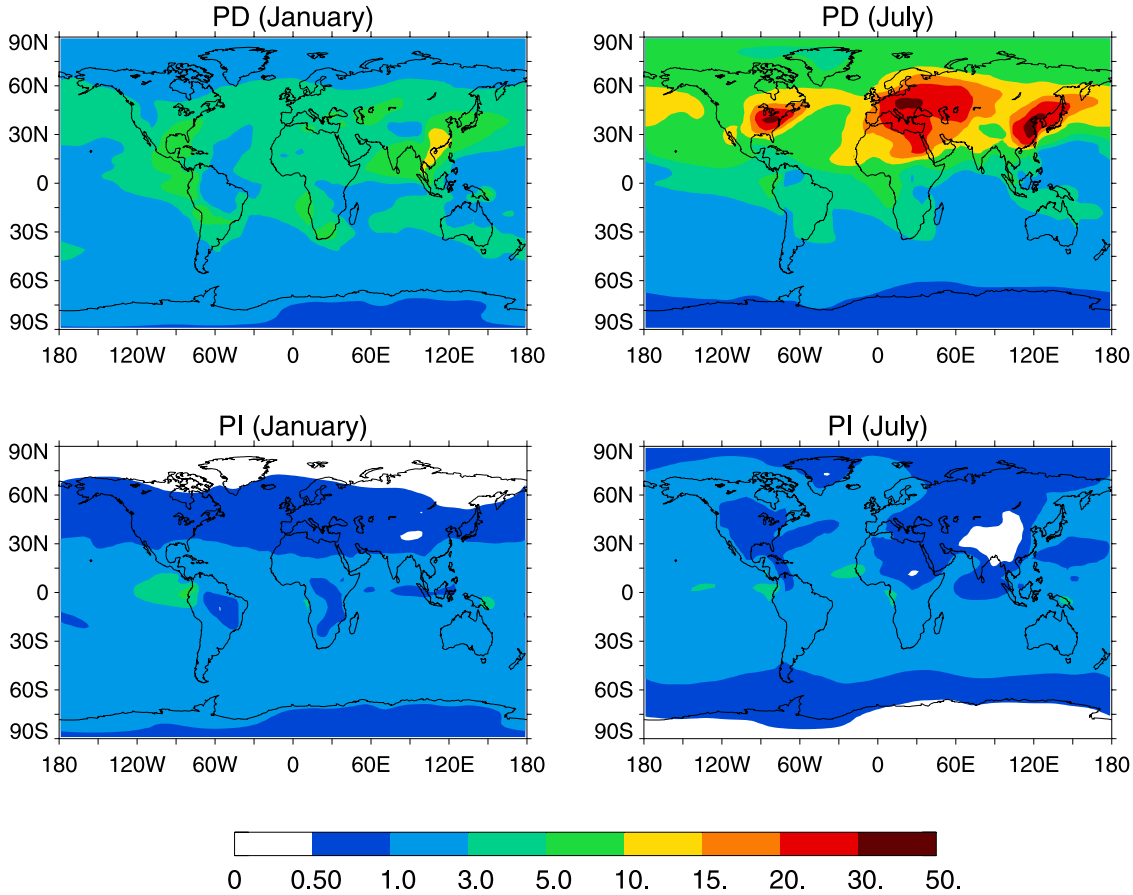

Figure 1. Present-day (PD) and preindustrial (PI) column burdens of sulfate aerosols (in mg m^{-2}) in January and July.

using another model, with substantially different cloud, aerosol and GCM physics representations.

3. Results

3.1. Aerosol Climatology

[14] Figure 1 plots the PD and PI column burdens of sulfate aerosol (SO_4^{2-}) in January and July. For PD, anthropogenic emissions significantly elevate sulfate burdens, especially in the Northern Hemisphere (NH), as compared to PI. The highest burdens are located largely over the source regions, namely, east Asia, Europe and northeast United States, because of the relatively short lifetime of sulfate aerosol. Seasonal variations are evident: the burdens in July are substantially higher than in January. The global annual mean sulfate burden is 0.22 Tg S for PI and 0.81 Tg S for PD, both of which are within the ranges reported in the literature (Table 1). The anthropogenic sulfate burden of 0.59 Tg S is considerably higher than 0.30 Tg S in the CSIRO studies [*Rotstayn*, 1999; *Rotstayn and Penner*, 2001] and 0.37 Tg S given by *Kiehl et al.* [2000], but is comparable to or slightly lower than the three scenarios simulated using the ECHAM GCM with sulfate cycle and cloud physics coupled [*Lohmann and Feichter*, 1997].

[15] As dictated by the empirical relationship of *Boucher and Lohmann* [1995], the droplet number concentration depends solely on the mass concentration of sulfate aerosol (Figure 2). For PI, the concentrations at the pressure level of 904 mbar, where liquid clouds frequently form, range from 75 to 150 cm^{-3} over land, while they are usually below 100 cm^{-3} over ocean. The land-ocean contrast in NH is much more pronounced for PD. The concentrations over land are consistently over 150 cm^{-3}, and reach as high as 300–500 cm^{-3} over the three source regions in July. As a result of long-range transport, the oceans downwind of the sources, namely, North Atlantic and North Pacific, also undergo anthropogenic impacts with droplets increasing to over 100 cm^{-3}. The concentrations in the Southern Hemisphere (SH) increase modestly, but to a much lesser extent than in NH, because of the lack of strong anthropogenic emissions.

3.2. Comparison of Simulated PD Cloud Parameters With Satellite Measurements

[16] The GCM-predicted zonal mean PD liquid water path (LWP) over ocean is compared with the Special Sensor Microwave Imager (SSM/I) measurements [*Greenwald et al.*, 1995; *Weng and Grody*, 1994] in Figure 3. In January, the model overestimates LWP in the low latitudes and midlatitudes by 18% on average. The simulated LWP in July is in good agreement with the observations in SH and in the NH low latitudes, whereas the model significantly overestimates LWP by a factor of 3 in the NH midlatitudes. The discrepancies are partly due to the difficulties in retrievals from precipitating clouds. The International Sat-

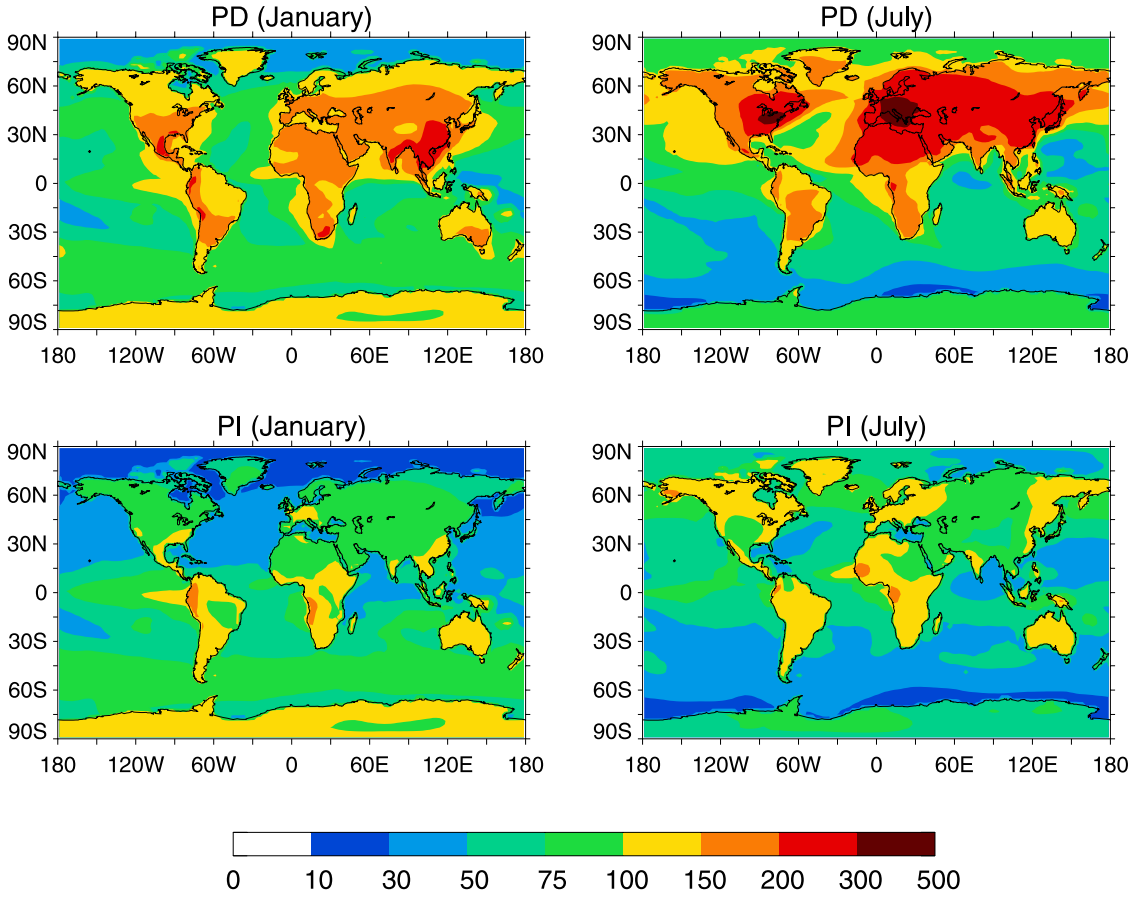

Figure 2. PD and PI droplet number concentrations (in cm^{-3}) at 904 mbar in January and July.

ellite Cloud Climatology Project (ISCCP) measurements of cloud optical depth are typically less than 5, and do not show the same pattern as the SSM/I measurements of LWP (Figure 4). The model simulations agree with the measurements within a factor of 2, except in the NH midlatitudes in July as a result of overestimated LWP.

[17] The GCM-predicted SW and LW cloud forcings are compared with the Earth Radiation Budget Experiment (ERBE) measurements in Figures 5 and 6, respectively. The model simulations generally achieve a good agreement with the measurements. However, a considerable discrepancy of 38 W m^{-2} in the SW cloud forcing occurs at 60°N in July when the model predicts exceptionally high LWP.

3.3. First Indirect Forcing

[18] As compared to PI, the higher droplet numbers of PD decrease cloud effective radii at a constant LWP, and subsequently increase reflected radiation, resulting in negative forcing. The GCM simulations show that the first indirect forcing is all in SW with an annul mean value of -1.5 W m^{-2} (Table 3). The seasonal variations in the droplet number concentration lead to a mean forcing of -1.0 W m^{-2} in January and -1.9 W m^{-2} in July. The cooling effect lies largely in NH, where most anthropogenic sources of sulfate aerosol are concentrated. The mean forcing is -2.3 W m^{-2} in NH and -0.6 W m^{-2} in SH.

[19] The geographical distribution of the first indirect forcing is plotted in Figure 7. Though most anthropogenic aerosols originate from the continents in NH, the cooling over ocean (-1.6 m^{-2}) is stronger than over land (-1.2 m^{-2}) mainly because of three reasons. First, driven by wind, the long-range transport of aerosols considerably increases droplet numbers over the oceans near to the sources. This explains why the oceanic regions off the coasts of east Asia and northeast United States claim some of the strongest cooling, consistent with *Jones et al.* [2001]. Second, clouds form more frequently over ocean, just off coastlines. This factor is illustrated by the strong cooling off the west coasts of North America and Africa due to the large amount of marine stratocumulus. Third, because of the nature of the empirical relationship of *Boucher and Lohmann* [1995], the clouds over ocean are more susceptible to the change in the mass concentration of sulfate aerosol than over land.

3.4. Flux Changes

[20] The second indirect effect results from the lengthening of cloud lifetime as anthropogenic aerosols can suppress rainfall, a process better characterized as response of the model as opposed to "forcing," since its occurrence relies in general on alteration of the meteorological fields. In light of this subtlety, the radiative flux changes at the top of the atmosphere (TOA) are often employed to gauge the sign and scale of the second indirect effect and, in some cases, those of the first indirect effect. *Rotstayn and Penner* [2001] termed this as "quasi forcing" whereas we prefer to term

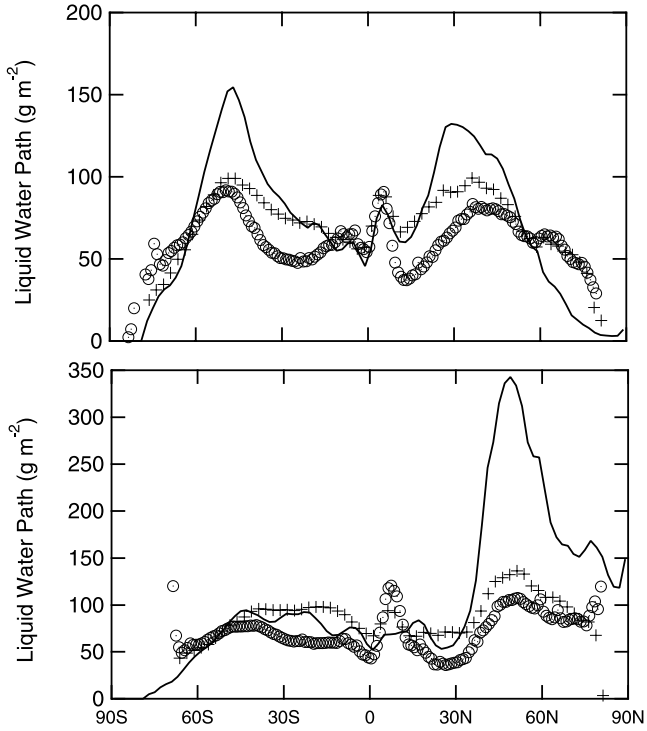

Figure 3. Zonal mean liquid water path over ocean in (top) January and (bottom) July simulated by general circulation model (GCM) (solid lines) and inferred from Special Sensor Microwave Imager measurements (crosses [*Greenwald et al.*, 1995] and circles [*Weng and Grody*, 1994]).

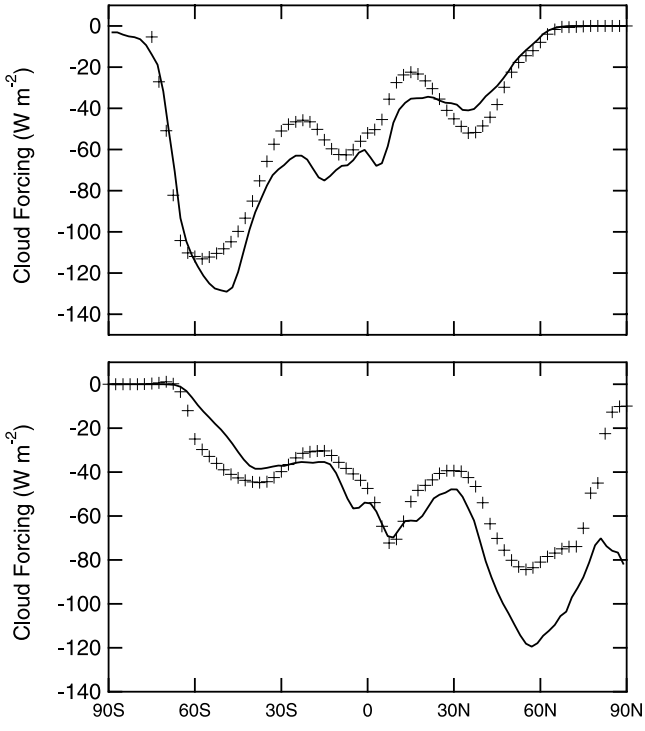

Figure 5. Zonal mean shortwave (SW) cloud forcing in (top) January and (bottom) July simulated by GCM (solid lines) and inferred from Earth Radiation Budget Experiment (ERBE) measurements (crosses).

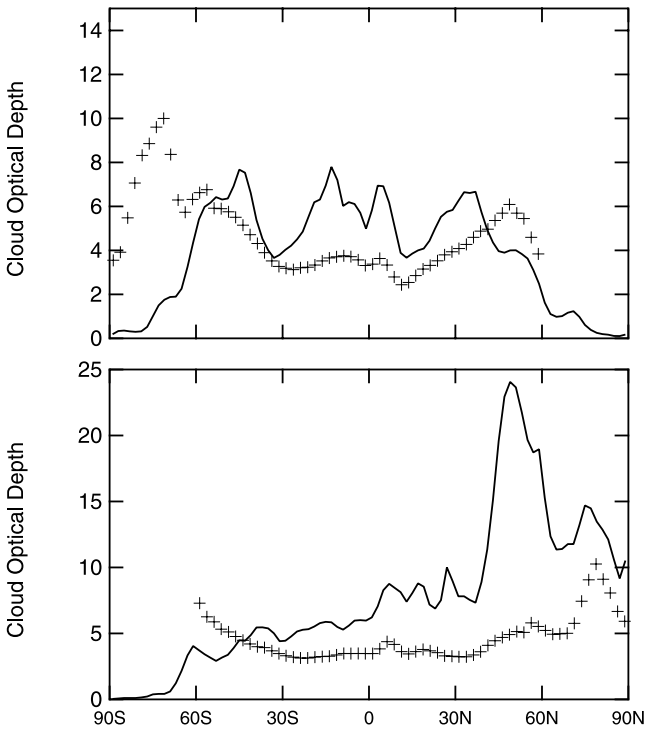

Figure 4. Zonal mean cloud optical depth in (top) January and (bottom) July simulated by GCM (solid lines) and inferred from International Satellite Cloud Climatology Project measurements (crosses).

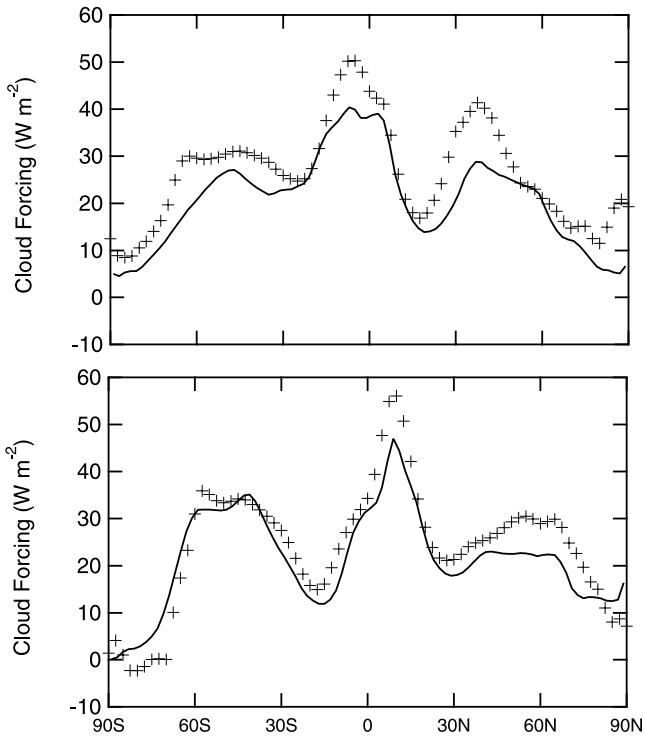

Figure 6. Zonal mean longwave (LW) cloud forcing in (top) January and (bottom) July simulated by GCM (solid lines) and inferred from ERBE measurements (crosses).

Table 3. Mean Forcing and Flux Changes[a]

	Annual Global	January	July	NH	SH	Land	Ocean
First indirect forcing	−1.5 (−1.5)	−1.0 (−1.0)	−1.9 (−1.9)	−2.3 (−2.3)	−0.6 (−0.6)	−1.2 (−1.2)	−1.6 (−1.6)
Flux change due to the first indirect effect	−1.4 (−1.6)	−1.0 (−0.7)	−1.4 (−1.8)	−2.3 (−2.4)	−0.6 (−0.7)	−1.2 (−1.5)	−1.5 (−1.6)
Flux change due to the second indirect effect	−0.9 (−1.1)	−0.3 (−0.3)	−1.0 (−1.5)	−1.4 (−1.7)	−0.4 (−0.5)	−0.4 (−0.8)	−1.0 (−1.2)
Flux change due to the combined indirect effects	−2.3 (−2.7)	−1.8 (−1.7)	−2.9 (−3.5)	−3.6 (−4.1)	−1.1 (−1.3)	−1.7 (−2.3)	−2.6 (−2.8)

[a]Values are given in W m^{-2}; SW components are in parentheses.

this simply as flux change, in contrast to the "forcing." In order to assess the second indirect effect and facilitate comparisons with existing studies, we present the calculated flux changes from the GFDL GCM as well as a discussion of the statistical significance of the results.

[21] The flux changes due to the first indirect effect are plotted in Figure 8. Note that there are regions of positive flux changes, in addition to negative ones. Despite scattered regional and positive radiative fluxes, negative flux changes indicative of cooling dominate NH. The mean flux change in NH is −2.3 W m^{-2} (Table 3). The regions that undergo strongest radiative cooling generally agree with those suggested by the forcing calculation (Figure 7). Some areas in SH such as parts of Africa and Australia experience warming to different extents while the rest experience cooling. The mean flux change in SH is −0.6 W m^{-2} (Table 3), suggesting that the warming and cooling largely cancel out.

[22] Figure 9 illustrates the geographical distribution of the SW and LW components of the flux changes due to the first indirect effect. A comparison of the SW flux changes with radiative forcing (which is in SW spectrum by definition) shows a general strengthening of SW cooling due to the model's response in the NH midlatitudes. In contrast to fixed cloud distributions used in computing forcing, the rearranged cloud fields give rise to changes in clouds and LW radiation. The LW flux changes are largely warming over the regions where the strongest SW cooling is located and thus mitigates that cooling. In terms of annual global means, the flux change due to the first indirect effect (−1.4 W m^{-2}) is very close to the first indirect forcing (−1.5 W m^{-2}), but this is partly due to offsets of flux changes of opposite signs and in different wavelengths, as opposed to the forcing, when the change is negative everywhere and solely in SW. It must be noted that this characteristic could differ considerably from one model to another depending on model response (particularly cloud feedbacks). Thus far, our study based on the GFDL GCM agrees with *Rotstayn and Penner* [2001] based on the CISRO GCM in suggesting the similarity of flux changes to "forcing" in the global mean. However, such a result could depend heavily on the physics parameterization (especially cloud physics) in the GCMs.

[23] Over the oceans in NH, the second indirect effect biases the flux changes toward negative, especially over North Atlantic (Figure 10). This is confirmed by the mean flux change in NH (−1.4 W m^{-2}) (Table 3). Large parts of North Pacific and Europe undergo modest warming as the model is allowed to respond to the change in the cloud droplet number concentration. Despite negligible difference in cloud cover, the average increase in cloud water amounts to 13%. As discussed later, the flux changes due to the second indirect effect are subject to large model natural variations, and thus the interpretation requires extra caution.

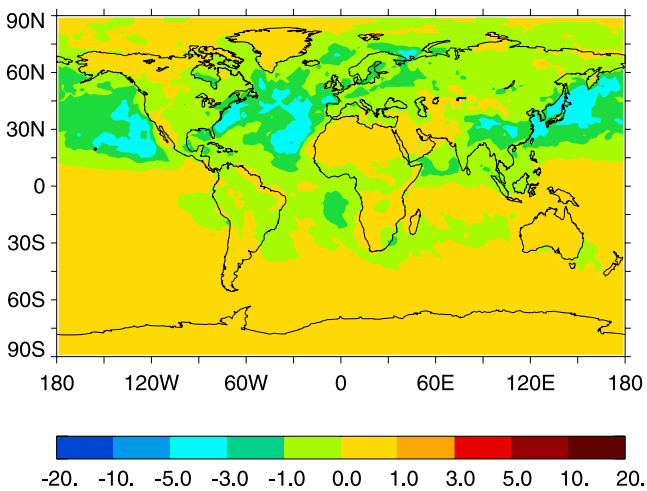

Figure 7. Geographical distribution of the annual mean first indirect forcing (in W m^{-2}).

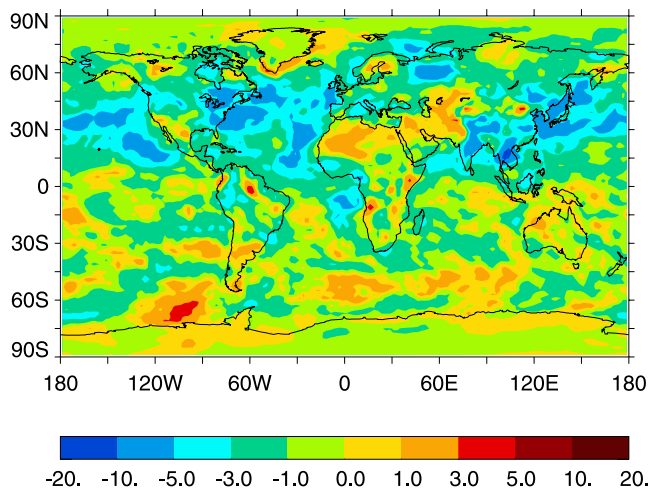

Figure 8. Geographical distribution of the annual mean flux changes (in W m^{-2}) due to the first indirect effect.

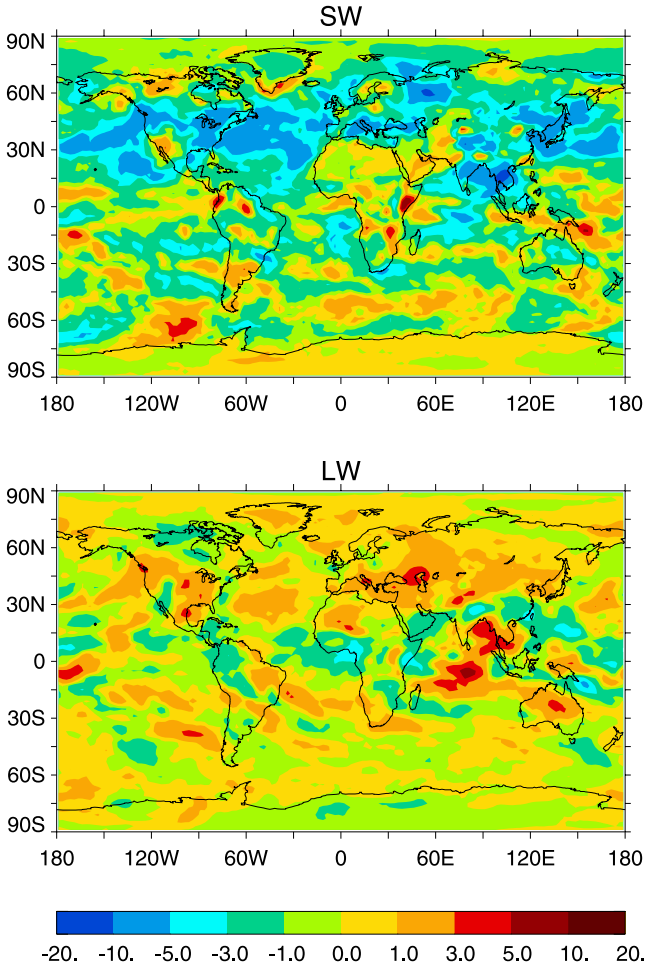

Figure 9. Geographical distribution of the SW and LW components of the annual mean flux changes (in W m^{-2}) due to the first indirect effect.

[24] As shown in Figure 11, a combination of the first and second indirect effects significantly strengthens the cooling in NH, especially over the oceans, leading to a mean flux change of −3.6 W m^{-2} (Table 3). The continental emission

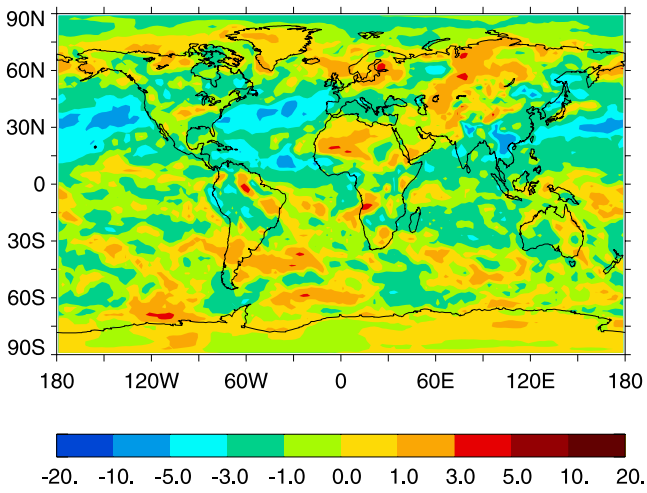

Figure 10. Geographical distribution of the annual mean flux changes (in W m^{-2}) due to the second indirect effect.

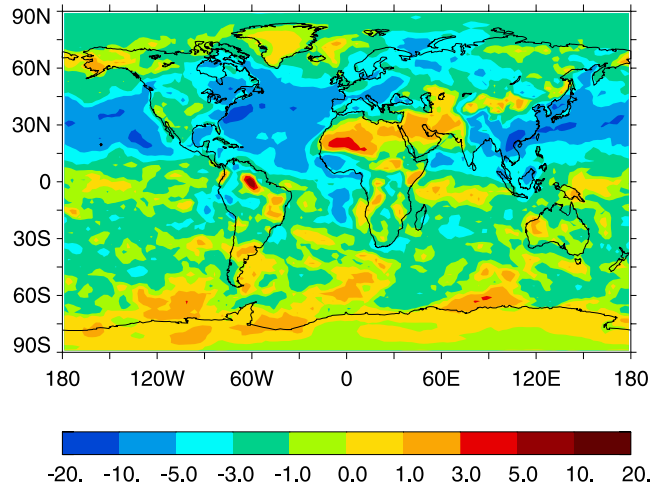

Figure 11. Geographical distribution of the annual mean flux changes (in W m^{-2}) due to the combined first and second indirect effect.

source regions register strong cooling, too. In terms of the global mean flux change, the combined effects result in −2.3 W m^{-2}, which is approximately equal to the linear addition of both effects. This is also true for the zonal mean in most latitudes.

[25] The key issue underlying the feasibility of using flux change as a tool to assess indirect effects is whether as a result of all kinds of feedback mechanisms in GCM (especially cloud feedbacks in the context of the present study), the natural variations in flux changes will overwhelm the possible signals of indirect effects. By conducting simulations of multiple years with the same yearly cycle of aerosol climatology, we find that the standard deviation of the annual global mean flux change (a measurement of variations) stands at 0.28 W m^{-2}. The calculated global mean flux changes all exceed the standard deviation, an indication of their statistical significance in all cases.

[26] The estimated standard deviations in annual zonal mean flux changes are plotted in Figure 12. The model exhibits relatively strong natural variations (>1 W m^{-2}) near to the equator and in the high latitudes of both hemispheres, while the variations normally stay below 1 W m^{-2} in the midlatitudes. Except in some NH low latitudes and midlatitudes, the GCM-simulated flux changes due to the second indirect effect are largely within one standard deviation of variations, meaning that the probabilities of them being due to model fluctuations are more than 68%. In comparison, the first indirect effect gives rise to stronger flux changes than the second indirect effect, exceeding the model variations in almost all NH low latitudes and midlatitudes. The fact that the flux changes due to the combined effects consistently exceed the model's natural variations in the whole NH and in most SH low latitudes and midlatitudes greatly strengthens the statistical significance of the estimates of the simulated total indirect radiative effects.

4. Discussion

[27] The previous GCM studies of indirect effects based on the relationship of *Boucher and Lohmann* [1995] are

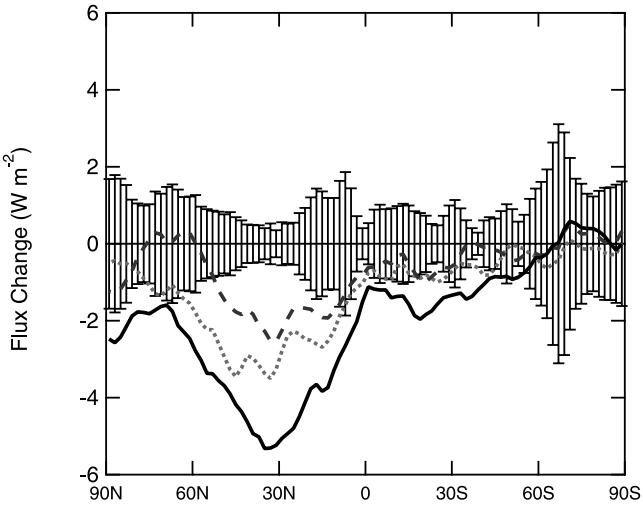

Figure 12. Annual zonal mean flux changes (in W m^{-2}) due to the first (dotted line), second (dashed line) and combined (solid line) indirect effects. The standard deviations of the natural variations of the model are represented by the error bars.

compared with this study in Table 1. This study obtains an annual mean forcing of -1.5 W m^{-2} and a flux change of -1.4 W m^{-2} due to the first indirect effect. The PI to PD increase in sulfate burden is 0.59 Tg S. In comparison, both estimates of *Boucher and Lohmann* [1995] with two different GCMs are -1.0 W m^{-2} from a burden increase of 0.44 Tg S. An increase of 0.38 Tg S results in an estimate of -0.8 W m^{-2} by parameterizing cloud amount according to *Sundqvist et al.* [1989] and autoconversion according to *Beheng* [1994] [*Feichter et al.*, 1997]. When the same cloud scheme is coupled with sulfur cycle, anthropogenic sulfate burden increases to 0.69 Tg S, and the forcing to -1.0 W m^{-2} [*Lohmann and Feichter*, 1997]. The flux change estimate and burden increase given by *Rotstayn* [1999] are -1.2 W m^{-2} and 0.3 Tg S, respectively. *Rotstayn and Penner* [2001] used a similar cloud scheme, but a different parameterization of autoconversion, and reported a flux change of -1.5 W m^{-2} from a burden of 0.3 Tg S. *Kiehl et al.* [2000] reported a forcing of -1.8 W m^{-2} from a burden of 0.37 Tg S. Because of the nonlinearity of the mechanisms associated with indirect effects, the concept of normalized forcing (i.e., forcing resulting from per unit burden) may not be as well applicable to indirect effects as to direct effects as given by *Ramaswamy et al.* [2001]. So, we only qualitatively point out that the forcing strengths reported by *Rotstayn* [1999], *Rotstayn and Penner* [2001] and *Kiehl et al.* [2000] are among the strongest, while the other four studies including this one are roughly comparable to one another.

[28] The combined effects of -2.3 W m^{-2} estimated in this study are in the range of -1.4 to -4.8 W m^{-2} reported by *Lohmann and Feichter* [1997] depending on different parameterizations of cloud water and autoconversion, and is comparable to -2.1 W m^{-2} estimated by *Rotstayn* [1999] and -2.3 W m^{-2} estimated by *Rotstayn and Penner* [2001] in spite of different sulfate burdens. Again, by taking into account the corresponding increases in sulfate burdens, we find that one particular case given by *Lohmann and Feichter* [1997] (the combination of the parameterizations of *Xu and Randall* [1996] and *Beheng* [1994]) and *Rotstayn* [1999] give rise to forcing strength much stronger than the other studies. One of the possible reasons for the discrepancies is the different parameterizations of autoconversion, which plays a critical role in determining indirect effects as suggested by *Lohmann and Feichter* [1997] and, more recently, by *Rotstayn and Liu* [2005].

[29] Since all these studies employed the same empirical sulfate-droplet relationship [*Boucher and Lohmann*, 1995], one of the most important processes for determining the indirect radiative effects, the rather good agreement among some studies by no means implies a resolution of the problem, although the consistency increases slightly the confidence that some elements of the process are being captured well. Nonetheless, given a variety of differences among these studies in terms of GCM structure, cloud scheme and microphysics, and aerosol climatology, such an agreement does affirm the practicality of using the GFDL GCM as a tool for studying aerosol-cloud interactions. It also highlights the significance of a reliable prediction of the cloud droplet number concentration for narrowing down the uncertainty associated with the calculated indirect forcing. Additionally, despite the different empirical relationships used in calculating droplet numbers, the geographical distribution of the first indirect forcing as simulated here agrees excellently with the Hadley Center HadAM3 model [*Jones et al.*, 2001].

[30] Despite the large differences in cloud scheme and physics parameterization between the GFDL and CSIRO GCMs, this study reaches a conclusion similar to *Rotstayn and Penner* [2001] that, for the first indirect effect, the global mean flux change is close to the forcing counterpart. However, the geographical distributions differ to some extent, as the model is allowed to respond to external forcing in the context of flux change. It is reiterated that the nature of the response relies on model parameterization. This factor becomes critically important when considering the fact that the second indirect effect is indeed flux change, and by no means a forcing. Besides, the forcing per unit sulfate burden obtained in this study is only half of that of *Rotstayn and Penner* [2001].

[31] A detailed simulation of cloud activation reveals a highly nonlinear process controlled by a number of factors including the chemical compositions and size distributions of aerosols and updraft velocity [*Ming et al.*, 2005]. Though efficient CCN, sulfate aerosol only accounts for a fraction of dry aerosol mass. The rest consists of an array of chemical species with different chemical and surface properties (e.g., nitrate and organic compounds). Therefore a relationship using sulfate as the sole surrogate for all aerosol species like the one used in this study [*Boucher and Lohmann*, 1995] is probably not comprehensive enough to capture the complexity of the whole activation process. This limitation contributes to the uncertainties in the estimated forcing and flux changes. Another source of uncertainty for this study arises from using monthly mean aerosol concentrations. It was shown that compared to deriving time-variant aerosol concentrations from a coupled chemistry-climate model, this simplification can overestimate the first indirect

forcing by 20% because of the nonlinearity of the indirect effects [*Feichter et al.*, 1997].

5. Conclusions

[32] This study uses the GFDL GCM in conjunction with monthly mean sulfate climatology from the MOZART chemistry-transport model and relates cloud droplet number concentrations to sulfate mass concentrations using an empirical relationship [*Boucher and Lohmann*, 1995]. It predicts an annual global mean first indirect forcing of -1.5 W m^{-2} from an anthropogenic sulfate burden of 0.59 Tg S. Most of the cooling occurs in NH, where most anthropogenic sources of aerosol are located. Owing to long-range aerosol transport, higher cloud frequency and susceptibility, the cooling over ocean is stronger than over land, resulting in an ocean-to-land ratio of 1.3. Some of the strongest forcing is located off the coasts of east Asia, Europe, and northeast United States. As a result of persistent marine stratocumulus, the oceanic regions off the west coasts of Africa and North America are responsible for the rest.

[33] A distinction is made between "forcing" and flux change at TOA in this study as the latter is necessary for assessing the magnitudes of the second and total indirect effects. The annual mean flux change due to the first indirect effect is -1.4 W m^{-2}, similar to the annual mean forcing. As the model is allowed to respond to forcing, a rearrangement of cloud distribution gives rise to changes in longwave flux (smaller than solar flux changes). Hence the geographical nature of the radiation field differs from that of the forcing. The annual mean flux change due to the second indirect effect amounts to -0.9 W m^{-2}. Both effects are approximately linearly additive, and the combined annual mean flux change is -2.3 W m^{-2}, 77% of which is concentrated in NH.

[34] The analyses of the model's natural variations suggest that the GCM-simulated annual zonal mean flux changes due to the second indirect effect are partly overwhelmed by natural variations and have low statistical significance, while the total effect exceeds variations in the entire NH and in the SH low latitudes and midlatitudes (north of 45°S). The area of significance for the total effect is wider than for the first and second effects considered separately. Despite the significant differences in cloud schemes, this study is consistent with a number of previous studies based on the same sulfate-droplet relationship in terms of global mean flux change in watts per square meter for the total effect.

References

Beheng, K. D. (1994), A parameterization of warm cloud microphysical conversion processes, *Atmos. Res.*, *33*, 193–206.

Berry, E. X. (1967), Cloud droplet growth by collection, *J. Atmos. Sci.*, *24*, 688–701.

Boucher, O., and U. Lohmann (1995), The sulphate-CCN-cloud albedo effect—A sensitivity study with two general circulation models, *Tellus, Ser. B*, *47*, 281–300.

Boucher, O., H. Le Treut, and M. B. Baker (1994), Sensitivity of a GCM to changes in cloud droplet concentration, paper presented at AMS 8th Conference on Atmospheric Radiation, Am. Meteorol. Soc., Nashville, Tenn.

Chen, C., and W. R. Cotton (1987), The physics of the marine stratocumulus-capped mixed layer, *J. Atmos. Sci.*, *44*, 2951–2977.

Feichter, J., U. Lohmann, and I. Schult (1997), The atmospheric sulfur cycle in ECHAM-4 and its impact on the shortwave radiation, *Clim. Dyn.*, *13*, 235–246.

Greenwald, T. J., G. L. Stephens, S. A. Christopher, and T. H. Vonder Haar (1995), Observations of the global characteristics and regional radiative effects of marine cloud liquid water, *J. Clim.*, *8*, 2928–2946.

Hoowitz, L. W., et al. (2003), A global simulation of tropospheric ozone and related tracers: Description and evaluation of MOZART, version 2, *J. Geophys. Res.*, *108*(D24), 4784, doi:10.1029/2002JD002853.

Jones, A., D. L. Roberts, M. J. Woodage, and C. E. Johnson (2001), Indirect sulphate aerosol forcing in a climate model with an interactive sulphur cycle, *J. Geophys. Res.*, *106*, 20,293–20,310.

Khairoutdinov, M., and Y. Kogan (2000), A new cloud physics parameterization in a large-eddy simulation model of marine stratocumulus, *Mon. Weather Rev.*, *128*, 229–243.

Kiehl, J. T., T. L. Schneider, P. J. Rasch, M. C. Barth, and J. Wong (2000), Radiative forcing due to sulfate aerosols from simulations with the National Center for Atmospheric Research Community Climate Model, version 3, *J. Geophys. Res.*, *105*, 1441–1457.

Le Treut, H., and Z. X. Li (1991), Sensitivity of an atmospheric general circulation model to prescribed SST changes: Feedback effects associated with the simulation of cloud optical properties, *Clim. Dyn.*, *5*, 175–187.

Lohmann, U., and J. Feichter (1997), Impact of sulfate aerosols on albedo and lifetime of clouds: A sensitivity study with the ECHAM4 GCM, *J. Geophys. Res.*, *102*, 13,685–13,700.

Lohmann, U., and J. Feichter (2004), Global indirect aerosol effects: A review, *Atmos. Chem. Phys. Discuss.*, *4*, 7561–7614.

Lohmann, U., and E. Roeckner (1996), Design and performance of a new microphysical scheme developed for the ECHAM general circulation model, *Clim. Dyn.*, *12*, 557–572.

Manton, M. J., and W. R. Cotton (1977), Formulation of approximate equations for modeling moist deep convection on the mesoscale, *Atmos. Sci. Pap. 266*, 62 pp., Dep. of Atmos. Sci., Colo. State Univ., Fort Collins.

Martin, G. M., D. W. Johnson, and A. Spice (1994), The measurement and parameterization of effective radius of droplets in warm stratocumulus clouds, *J. Atmos. Sci.*, *51*, 1823–1842.

Ming, Y., V. Ramaswamy, L. J. Donner, and V. T. J. Phillips (2005), A robust parameterization of cloud droplet activation, *J. Atmos. Sci.*, in press.

Ramaswamy, V., et al. (2001), Radiative forcing of climate change, in *Climate Change 2001, The Scientific Basis, Contribution of Working Group I to the Third Assessment Report of the Intergovernmental Panel on Climate Change*, edited by J. T. Houghton et al., pp. 349–416, Cambridge Univ. Press, New York.

Rasch, P. J., and J. E. Kristjánsson (1998), A comparison of the CCM3 model climate using diagnosed and predicted condensate parameterizations, *J. Clim.*, *11*, 1587–1614.

Roeckner, E., M. Rieland, and E. Keup (1991), Modelling of clouds and radiation in the ECHAM model, paper presented at ECMWF/WCRP Workshop on Clouds, Radiative Transfer and the Hydrological Cycle, Eur. Cent. for Medium-Range Forecasts, Reading, U.K.

Rotstayn, L. D. (1997), A physically based scheme for the treatment of stratiform clouds and precipitation in large-scale models. I: Description and evaluation of microphysical processes, *Q. J. R. Meteorol. Soc.*, *123*, 1227–1282.

Rotstayn, L. D. (1999), Indirect forcing by anthropogenic aerosols: A global climate model calculation of the effective-radius and cloud-lifetime effects, *J. Geophys. Res.*, *104*, 9369–9380.

Rotstayn, L. D. (2000), On the "tuning" of autoconversion parameterizations in climate models, *J. Geophys. Res.*, *105*, 15,495–15,507.

Rotstayn, L. D., and Y. Liu (2005), A smaller global estimate of the second indirect aerosol effect, *Geophys. Res. Lett.*, *32*, L05708, doi:10.1029/2004GL021922.

Rotstayn, L. D., and J. E. Penner (2001), Indirect aerosol forcing, quasi forcing, and climate response, *J. Clim.*, *14*, 2960–2975.

Rotstayn, L. D., B. F. Ryan, and J. Katzfey (2000), A scheme for calculation of the liquid fraction in mixed-phase clouds in large-scale models, *Mon. Weather Rev.*, *128*, 1070–1088.

Slingo, A. (1989), A GCM parameterization for the shortwave radiative properties of water clouds, *J. Atmos. Sci.*, *46*, 1419–1427.

Smith, R. N. B. (1990), A scheme for predicting layer clouds and their water content in a general circulation model, *Q. J. R. Meteorol. Soc.*, *116*, 435–460.

Sundqvist, H. (1978), A parameterization scheme for non-convective condensation including prediction of cloud water content, *Q. J. R. Meteorol. Soc.*, *104*, 677–690.

Sundqvist, H., E. Berge, and J. E. Kristjánsson (1989), Condensation and cloud parameterization studies with a mesoscale numerical weather prediction model, *Mon. Weather Rev.*, *117*, 1641–1657.

The GFDL Global Atmospheric Model Development Team (2004), The new GFDL global atmosphere and land model AM2-LM2: Evaluation with prescribed SST simulations, *J. Clim.*, *17*, 4641–4673.

Tie, X., G. Brasseur, L. Emmons, L. Horowitz, and D. Kinnison (2001), Effects of aerosols on tropospheric oxidants: A global model study, *J. Geophys. Res.*, *106*, 22,931–22,964.

Tie, X., S. Madronich, S. Walters, D. P. Edwards, P. Ginoux, N. Mahowald, R. Zhang, C. Lou, and G. Brasseur (2005), Assessment of the global impact of aerosols on tropospheric oxidants, *J. Geophys. Res.*, *110*, D03204, doi:10.1029/2004JD005359.

Tiedtke, M. (1993), Representation of clouds in large-scale models, *Mon. Weather Rev.*, *121*, 3040–3061.

Xu, K. M., and D. A. Randall (1996), A semiempirical cloudiness parameterization for use in climate models, *J. Atmos. Sci.*, *53*, 3084–3102.

Weng, F., and N. G. Grody (1994), Retrieval of cloud liquid water using the Special Sensor Microwave/Imager (SSM/I), *J. Geophys. Res.*, *99*, 25,535–25,551.

P. A. Ginoux, L. W. Horowitz, and V. Ramaswamy, Geophysical Fluid Dynamics Laboratory, Princeton, NJ 08542, USA. (paul.ginoux@noaa.gov; larry.horowitz@noaa.gov; v.ramaswamy@noaa.gov)

Y. Ming, Visiting Scientist Program, University Corporation for Atmospheric Research, Geophysical Fluid Dynamics Laboratory, Princeton, NJ 08542, USA. (yi.ming@noaa.gov)

L. M. Russell, Scripps Institute of Oceanography, University of San Diego, La Jolla, CA 92093, USA. (lmrussell@ucsd.edu)